Clim Dyn (2011) 36:711–726
DOI 10.1007/s00382-009-0651-3

Precipitation in the Anatolian Peninsula: sensitivity to increased SSTs in the surrounding seas

Deniz Bozkurt · Omer Lutfi Sen

Received: 27 June 2009 / Accepted: 10 August 2009 / Published online: 23 August 2009

Abstract Effects of the increased sea surface temperatures (SSTs) in the surrounding seas of the Anatolian Peninsula on the precipitation it receives are investigated through sensitivity simulations using a state-of-the-art regional climate model, RegCM3. The sensitivity simulations involve 2-K increases to the SSTs of the Aegean, eastern Mediterranean and Black seas individually as well as collectively. All the simulations are integrated over a 10-year period between 1990 and 2000. The model simulations of this study indicate that the precipitation of the peninsula is sensitive to the variations of the SSTs of the surrounding seas. In general, increased SSTs lead to increases in the precipitation of the peninsula as well as that of the seas considered. The statistically significant increases at 95% confidence levels largely occur along the coastal areas of the peninsula that are in the downwind side of the seas. Significant increases do also take place in the interior areas of the peninsula, especially in the eastern Anatolia in winter. The simulations reveal that eastern Mediterranean Sea has the biggest potential to affect the precipitation in the peninsula. They also demonstrate that taking all three seas into account simultaneously enhances the effect of SSTs on the peninsula's precipitation, and extends the areas with statistically significant increases.

Keywords Anatolian Peninsula · Climate · Sea surface temperature · Regional climate modeling · RegCM3

D. Bozkurt · O. L. Sen (✉)
Eurasia Institute of Earth Sciences, Istanbul Technical University, Maslak, 34469 Istanbul, Turkey
e-mail: senomer@itu.edu.tr

1 Introduction

Climate variability and climate change in the Mediterranean Basin have been of interest to many researchers (e.g., Bolle 2003; Giorgi and Lionello 2008; Onol and Semazzi 2009; Evans 2009) as the basin lies in a transitional zone whose characteristics are determined by both mid-latitude and tropical variability. The Fourth Assessment Report of the Intergovernmental Panel on Climate Change (IPCC 2007) reveals that the Mediterranean Basin is one of the most vulnerable regions to the global climate change. GCM (General Circulation Model) climate change simulations for various emission scenarios point out significant basin-wide reductions in precipitation besides increases in temperatures by the end of the twenty-first century (IPCC 2007). Downscaling studies (e.g., Gao et al. 2006; Bozkurt et al. 2008; Onol and Semazzi 2009), providing greater detail for the region, demonstrate that the reductions are more pronounced along the coastal areas. Intriguingly, just to the north of the basin, e.g., the Alps, the Carpathians, the Black Sea Basin and the Caucasus mountains, the same studies generally indicate increases in precipitation. The drying in the Mediterranean is explained with strengthening of the anticyclonic circulation while the increase to the north is interpreted with a poleward shift in the Atlantic storm tracks (Giorgi and Lionello 2008).

There are several diagnostic studies that focus on large-scale circulation patterns and atmospheric teleconnections (e.g., Rodo et al. 1997; Trigo et al. 2000; Maheras et al. 2001; Xoplaki et al. 2004; Trigo et al. 2006), and they are important in understanding the climate variability in the Mediterranean basin. Studies concerning the relationship between sea surface temperature (SST) and precipitation variability have mostly concentrated on the tropical oceans (e.g., Arpe et al. 1998; Janicot et al. 1998; Messager et al.

2004). It is only recently that studies for the relationship between SST and climate variability have been done for the Mediterranean region. Li (2006) studied the atmospheric response to an idealized 2 K cooling of the Mediterranean Sea with a GCM, and he demonstrated large-scale changes in the atmospheric circulation to this cooling. He hypothesized that the Mediterranean Sea could initiate atmospheric teleconnections, and thus influence the weather and the climate of the remote regions. Rowell (2003) also investigated the role of the Mediterranean Sea in the Sahelian rainfall season with a GCM. He indicated that an increase in moisture transport in the eastern part of the Sahara due to warmer Mediterranean Sea results in an increase in the Sahelian summer rainfall. Maracchi et al. (1999) investigated how SST of Tyrrhenian Sea, a subdivision of the Mediterranean Sea, triggered convective precipitation in Tuscany, Italy. They analyzed four local-scale extreme convective events resulted in flash floods, gusts, and tornado-like systems in Tuscany region. According to their results, there is a positive correlation between SST anomalies of the Ligurian Gulf and frequency and intensity of extreme convective events in Tuscany region.

Anatolia (also known as Asia Minor), a peninsula in the eastern Mediterranean, is surrounded by Black Sea in the north, Aegean Sea in the west and Mediterranean Sea in the south (Fig. 1). It comprises most of Turkey. The terrain of the peninsula is quite complex, and together with its surroundings it shows some remarkable contrasting features in topography, land-sea boundary and landscape. The coastal areas demonstrate the characteristics of Mediterranean climate with some variations while the interior plateau indicates the attributes of the continental climate. Annual precipitation in the Aegean and Mediterranean coasts varies from 600 to 1,300 mm. Due to the orographic effect by the steep topography, eastern coast of the Black Sea receives the greatest amount of annual rainfall in the peninsula (over 2,000 mm). The annual precipitation in the Central Anatolia is comparatively small, averaging about 400 mm.

Anatolian Peninsula (hereafter AP) is under the influence of polar air masses in winter and tropical air masses in summer. In the cold half of the year (October to March), maritime polar air masses from the Atlantic with a track over Eastern Europe favor the cyclogenesis over the eastern Mediterranean and Aegean Sea (Lionello et al. 2006; Romem et al. 2007). The cyclones over Aegean Sea tend to follow two paths, one towards northeast affecting the northwestern parts of the peninsula (especially Marmara Sea and surrounding areas), and the other towards east taking the advantage of the east-west oriented valleys to penetrate interior areas of the AP (Karaca et al. 2000). Apart from these, there is also a more southerly trajectory over Mediterranean Sea followed by cyclones that influence the southern sea facing sides and eastern parts of the peninsula. It is also reported that a cyclone moving along the Mediterranean coast of the peninsula produces a secondary lee trough along the Black Sea coast (Brody and Nestor 1980). In addition, a track of continental polar with strong northeasterly winds over the temperate Black Sea surface supplies considerable moisture and heat to form precipitation, often in the form of snow, along the Black Sea coasts (Tayanc et al. 1998; Kindap 2009). The moisture laden maritime tropical air masses cross the Mediterranean Sea and causes rainfall events, especially in the western parts. If the dry but warm African air (continental

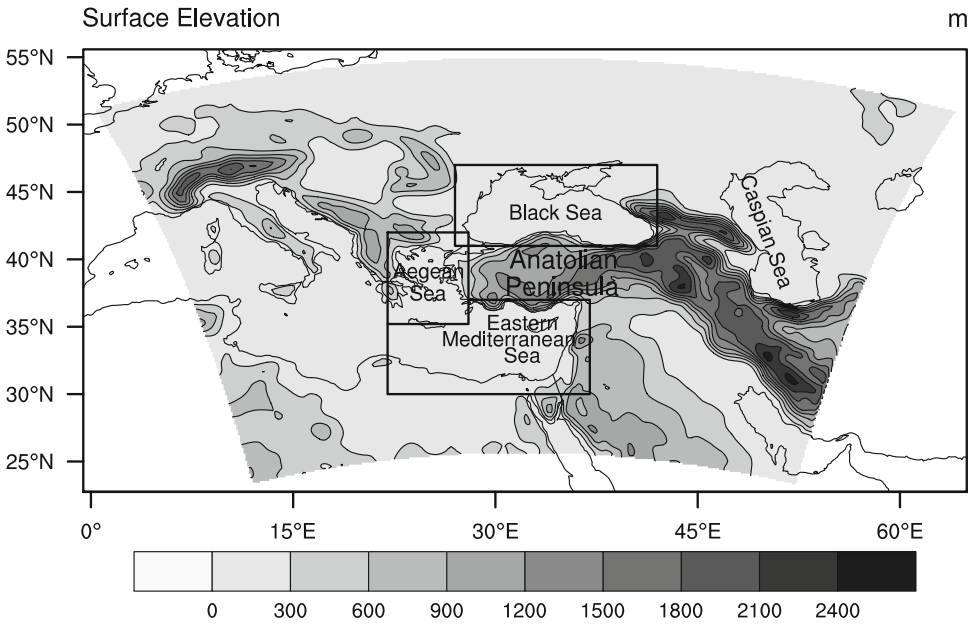

Fig. 1 Topography in the model domain, and the three surrounding seas of Anatolian Peninsula in which sea surface temperatures are modified

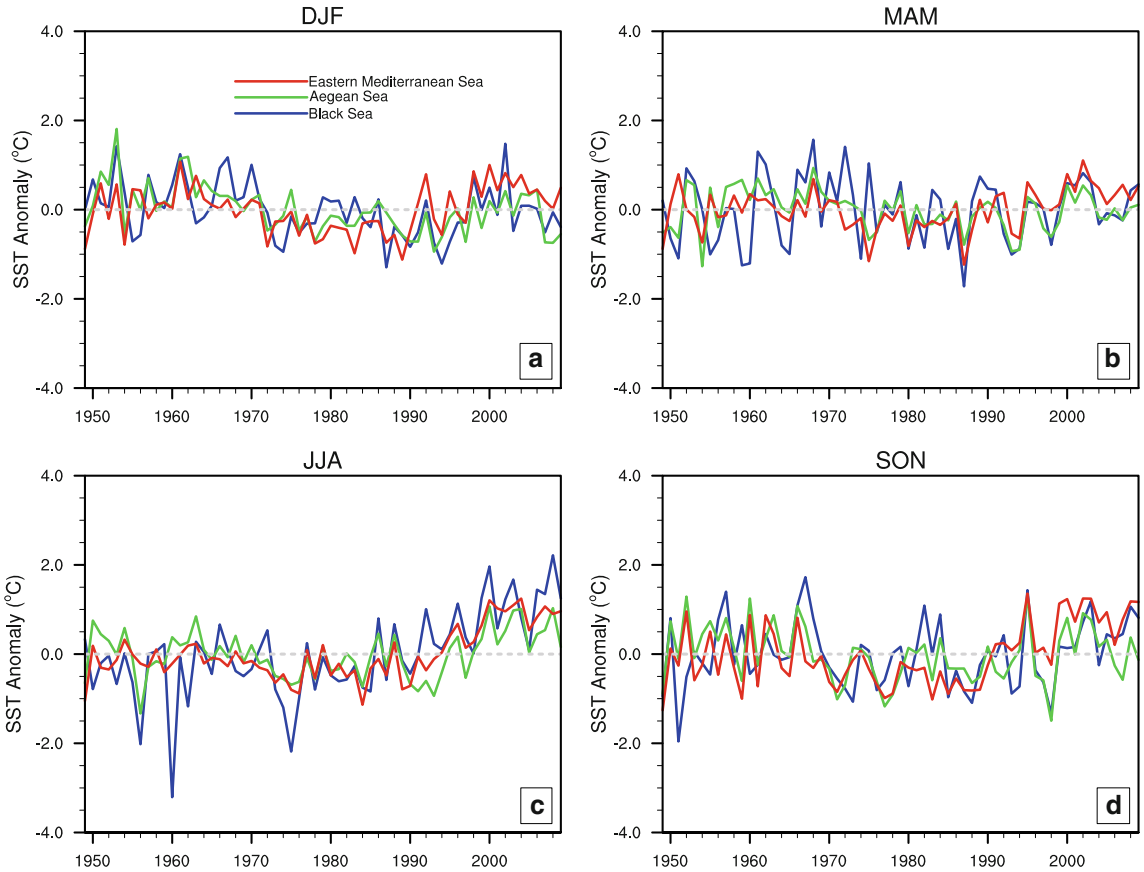

Fig. 2 Yearly variations in seasonal sea surface temperature (SST) anomalies of surrounding seas of the Anatolian Peninsula for the period 1949–2008. **a** For winter (DJF stands for December, January and February), **b** For spring (MAM is for March, April and May), **c** For summer (JJA is for June, July and August), and **d** For autumn (SON is for September, October and November)

tropical) follows a path over eastern Mediterranean Sea, it may cause rainfall with dust in the peninsula as well. The information given so far reveals that the majority of the air masses pass over the surrounding seas before reaching the AP. The question that is addressed here is, therefore, whether the surrounding seas have a noteworthy role on the seasonal precipitation in the peninsula.

Long-term variations (1949–2008) in seasonal SST anomalies of surrounding seas of the peninsula indicate a striking warming period beginning from the early 1990s (see Fig. 2), in parallel with the warming of the surface air as indicated by the station data in this region. The projections from the outputs of MPI's (Max Planck Institute) ECHAM5/MPI-OM and NCAR's (National Center for Atmospheric Research) CCSM models for the A2 scenario over eastern Mediterranean Sea indicate an increase in seasonal SST anomaly, approaching 2°C during the first half of the twenty-first century and 4°C in the late twenty-first century (see Fig. 3). The question that is addressed in this paper is therefore very relevant when considered from the perspective of warming seas in this region as well.

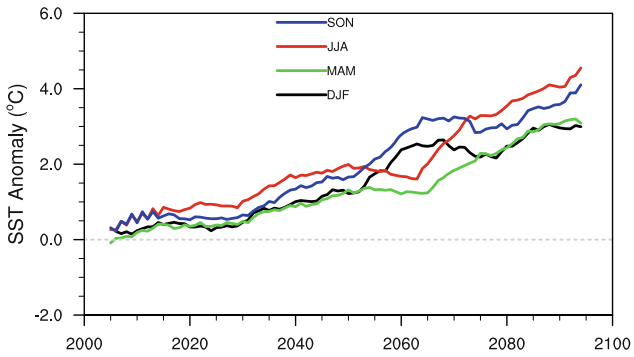

Fig. 3 Time series of the 10-year moving average of projected seasonal SST anomalies (differences from the 1961–1990 averages) for eastern Mediterranean Sea. The anomalies are obtained from the average of two climate change projections simulated by MPI's (Max Planck Institute) ECHAM5/MPI-OM and NCAR's (National Center for Atmospheric Research) CCSM models for the A2 scenario in an ongoing project supported by UNDP

An analysis based on long-term (1950–2001) time series of SSTs of the nearby seas and observed precipitation yields weak correlations across the AP (not shown here). This does not mean that the SSTs of nearby seas do not

have any impact on precipitation generating systems affecting the peninsula, it may rather mean that the SST signal from nearby seas in precipitation is relatively small and difficult to detect using this approach. Perhaps, the best way to assess the effect of SSTs on precipitation is to conduct model sensitivity experiments involving changes to SST values at certain sea regions. Therefore, we carried out sensitivity experiments involving +2 K perturbations using a state-of-the-art regional climate model, RegCM3. Further information about the model, data and experimental design of the simulations is given in Sect. 2. The performance of the model is evaluated in Sect. 3. Sensitivity experiment results are presented in Sect. 4. Finally, a summary and discussions are given in Sect. 5.

2 Model description, data, and experiment design

2.1 Model description

In this study, we deployed RegCM3, the regional climate model of the International Centre for Theoretical Physics in Italy. RegCM3 is an upgraded version of RegCM2 (Giorgi et al. 1993a, b), and it is a primitive equation, hydrostatic, compressible, limited area model with sigma-pressure vertical coordinate. RegCM3 includes the land surface model BATS (Biosphere–Atmosphere Transfer Scheme; Dickinson et al. 1993), the non local boundary layer scheme of Holtslag et al. (1990), the radiative transfer package of CCM3 (Community Climate Model Version 3; Kiehl et al. 1996), the ocean surface flux parameterization of Zeng et al. (1998), a simplified version of the explicit moisture scheme of Hsie et al. (1984), a large-scale cloud and precipitation scheme which accounts for the subgrid-scale variability of clouds (Pal et al. 2000), and several options for cumulus convection (Anthes 1977; Grell 1993; Emanuel and Zivkovic-Rothman 1999). In this study, we used the suggested parameterization schemes of the model for the mid latitudes involving Grell (1993) as cumulus convection scheme. Detailed descriptions of physical parameterizations and RegCM3 model can be found in Pal et al. (2007).

2.2 Data and experiment design

The modeling experiment consists of five 10-year simulations, for which RegCM3 was run with initial and boundary conditions provided by using the NCEP/NCAR Reanalysis data available at 6-h intervals with a resolution of $2.5^{o} \times 2.5^{o}$ in the horizontal and 17 pressure levels. Land use and vegetation data were derived from the Global Land Cover Characterization (GLCC) data at 10-min resolution. SSTs were obtained from the NOAA optimum interpolation SST analysis (Version 2) of Reynolds et al. (2002). The domain for simulations was centered at 40^{o}N and 32^{o}E with 144×110 grid cells with 30 km spatial resolution using a Lambert Conformal projection (Fig. 1). The simulations were performed continuously from 1 October 1990 to 31 December 2000. First 2 months (October and November) were selected as "spin-up" period, and thus, discarded in all simulations.

The modeling experiment includes a control simulation, used as reference, and four sensitivity simulations that involve perturbations to SSTs in certain regions. These regions are Aegean Sea (hereafter AS), eastern Mediterranean Sea (hereafter EMS) and Black Sea (hereafter BS). They are also considered together in the forth simulation. In the sensitivity simulations, SSTs of these regions are increased 2 K over those used in the control simulation.

SST perturbations of 2 K are used in several studies (e.g., Li 2006), but whether it is relevant for this region is assessed through checking long-term variations of seasonal SST anomalies in the three regions considered in this study (Fig. 2). All three seas show remarkable year-to-year and decadal variations. The year-to-year variation is larger in the BS, an inland sea, compared to those in the other two. This may be related to frequency of the overpassing atmospheric systems and the rivers such as the Don, Dnieper and Danube discharging large amounts of water into the BS that has positive water budget. The SST anomaly variations in the AS and EMS closely follow each other. In addition to substantial yearly variations, both seas indicate a multi-decadal variability, especially well indicated in winter. Starting early 1960s, a clear cooling trend lasts until 1990s, after when the SSTs show a strong warming trend. This cooling in about 30 years amounts to around 2 K. Such variations in addition to yearly ones reveal that the 2 K perturbation used in the sensitivity simulations is very relevant for this region. Projections of a warming climate in this region also strengthen this inference. Figure 3, for instance, demonstrates the projected changes in seasonal SST anomalies (differences from the 1961–1990 averages) for an area covering EMS. SST anomaly for each season increases throughout the twenty-first century based on IPCC's A2 emission scenario. Seasonal SST anomalies are projected to reach to about 3–4°C by the end of this century.

For model performance evaluation, the simulation results were compared with both the driving fields from NCEP/NCAR Reanalysis data and the station data provided by the State Meteorological Service of Turkey. Monthly mean, maximum and minimum temperatures and monthly precipitation data from 247 meteorological stations in and around the AP (see Fig. 4 for the distribution of the stations) were interpolated to the model grids via nearest neighborhood method. The gridded observations were then compared with the simulated monthly values to assess the model

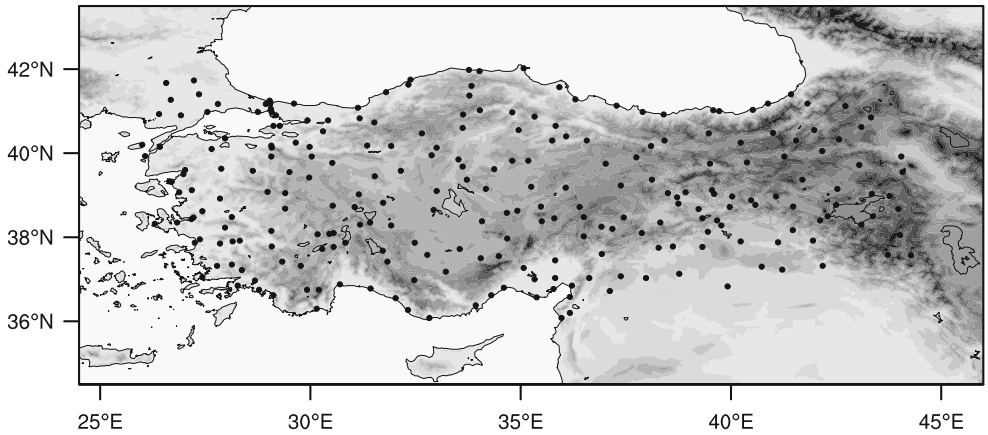

Fig. 4 Distribution of the 247 stations provided by the State Meteorological Service of Turkey

performance. Gokturk et al. (2008) provides detailed information about the quality control and homogeneity analysis of the observed precipitation data used in this study.

Because precipitation is the climate parameter that is in the focus of this study, here we primarily present the precipitation evaluation part of the model performance study. In order to assess how the SST perturbations affect the precipitation, we demonstrate seasonal average differences between the sensitivity simulations and the control simulation. Statistically significant changes in precipitation were determined using Student's t test with 95% confidence level for every model grid for each season, and the areas were hatched accordingly.

3 Model performance

It is conventional first to evaluate the performance of a climate model in terms of its ability to simulate the large-scale atmospheric fields, such as geopotential height, wind vectors, air temperature and specific humidity. Such an evaluation was also performed for the control simulation of this study. The atmospheric outputs of the simulation were compared with the driving fields from the NCEP/NCAR Reanalysis data. It is observed that RegCM3 is capable of simulating large-scale fields in the eastern Mediterranean quite well. The results of a study that includes the climate characteristics of this relatively less studied region and their simulation by RegCM3 are given in another article, which also includes the model's performance in simulating the large-scale atmospheric fields (Bozkurt et al. 2009). Therefore, here we prefer to concentrate on the performance analysis of precipitation as this parameter is in the focus of the present study. Because the direction and strength of the winds are important in interpreting the precipitation distribution in the AP, the seasonal 850 hPa wind vectors are also presented in the same figures with the precipitation.

Topography plays an important role in the distribution of precipitation in the AP. Sea facing sides of mountain ranges along the northern and southern coasts receive most of the precipitation. These mountain ranges limit the penetration of moisture laden air to the interior regions, therefore, the interior high plateau receives much less precipitation. The only path that allows moist air to reach to the central parts in large quantities is through the western side where the valleys between the mountain ranges that lie perpendicular to the AS coasts provide easy passages for westerly airflows.

Figure 5 shows the distributions of observed and simulated seasonal (averaged for 10 years) precipitation in Turkey, the country that covers almost the whole AP. Overall, the model reproduces the observed spatial patterns of precipitation in all seasons reasonably well. In winter, the observations illustrate the more typical distribution of precipitation in Turkey reflecting the effect of the topography and winds (Fig. 5a). The 850 hPa winds are northwesterly over the AS, and they are mostly westerly over the BS and EMS in this season (Fig. 5a). The model simulates both the wind patterns and the spatial distribution of the precipitation quite well (Fig. 5b). Table 1 provides some statistics for the model performance (Details of the statistics can be found in Wang et al. (2003)). For winter, the observed and model estimated average precipitation values for the whole area are close to each other; spatial correlation is calculated to be 0.60; and the spatial standard deviations of observed and estimated precipitation are also close to each other (see Table 1).

In spring, it is clearly seen that the model overestimates precipitation in the BS coasts of the AP, but it broadly captures the spatial distribution in other regions (Fig. 5c, d). These are also reflected in the statistical data given in Table 1. Spatial correlation for this season is low (0.44) compared to that for winter. The model also estimates a relatively larger spatial standard deviation. The 850 hPa

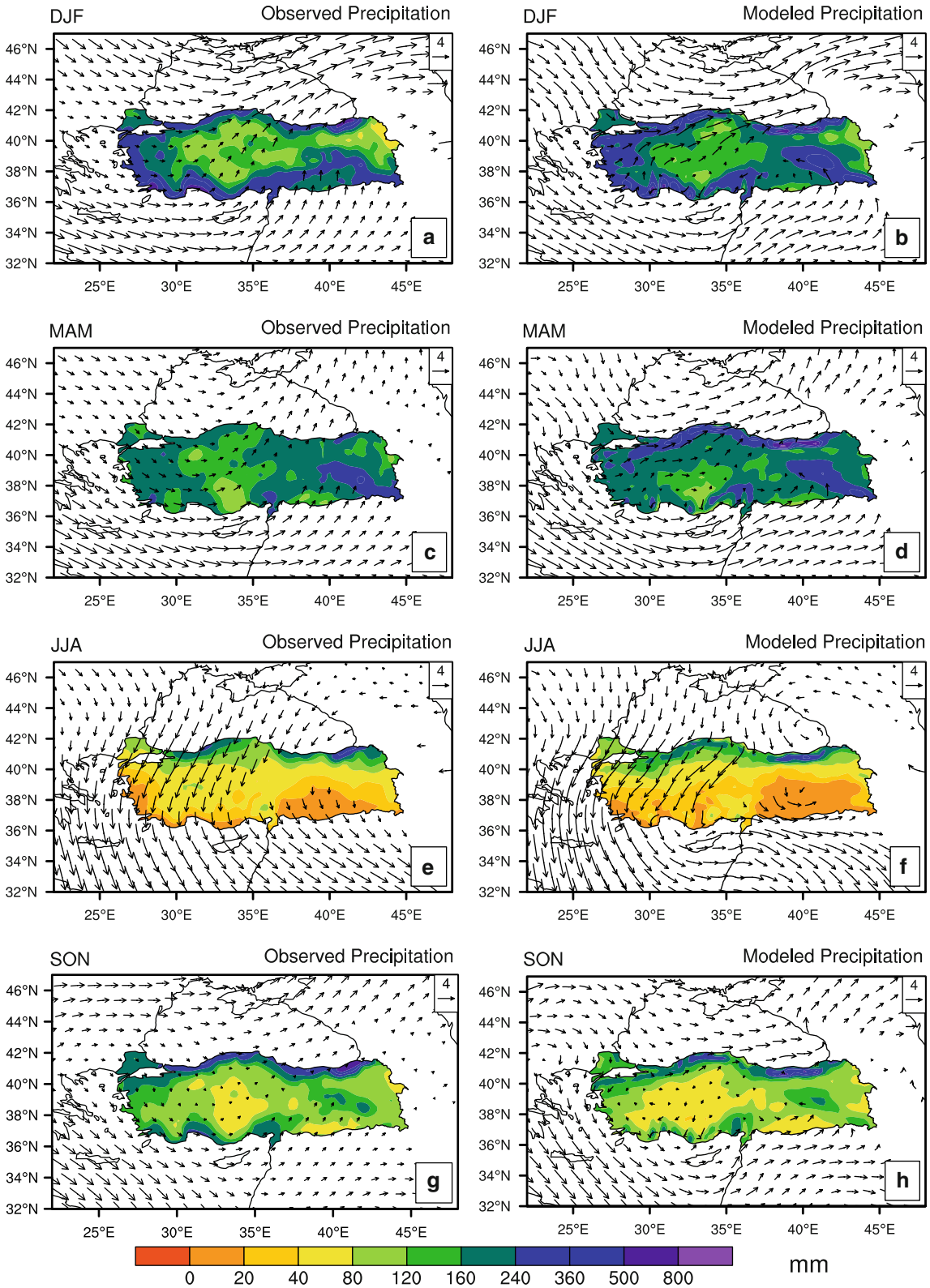

Fig. 5 10-year average spatial pattern of observed (*left*) and simulated (*right*) precipitation (mm) in Turkey for winter (DJF) (**a**, **b**), for spring (MAM) (**c**, **d**), for summer (JJA) (**e**, **f**) and for autumn (SON) (**g**, **h**). Also included 10-year seasonal average of 850 hPa wind vectors (m/s) from NCEP/NCAR Reanalysis (*left*) and control simulation (*right*)

Table 1 Seasonal statistics of observed and simulated precipitation (mm/day) in Turkey

Seasons	Observed (mm/day)	Estimated (mm/day)	Bias (mm/day)	SC	SSD (mm/day)	
					Observed	Estimated
DJF	2.36	2.39	0.03	0.60	1.13	0.93
MAM	2.01	2.27	0.26	0.44	0.53	0.77
JJA	0.72	0.62	−0.10	0.66	0.71	0.56
SON	1.57	1.20	−0.37	0.55	0.98	0.59

SC spatial pattern correlation coefficient, *SSD* spatial standard deviation

wind pattern in this season is quite similar to that in winter, but the winds are weaker over the BS and stronger over the AS and EMS. The model captures the pattern fairly well, but it simulates stronger winds over the BS, and this may be the part of the reason why it overestimates the precipitation along the BS coasts.

In summer, the BS coasts and northern parts of Turkey are the wettest regions (more than 100 mm) according to observations, and this feature is well simulated by the model (Fig. 5e, f). The relatively large spatial correlation (0.66) indicates that the model's performance for summer is fairly good (Table 1). Strong north-northeasterly winds at 850 hPa dominate the airflow in the BS and western parts of the AP in summer. The model simulates a cyclonic circulation over the eastern BS that results in northwesterly westerly airflow along the eastern coasts of the AP. This is probably the reason why that area receives relatively high amounts of precipitation in summer.

In autumn, the distribution of precipitation in Turkey looks more like that in winter but in less quantity (Fig. 5g). The model reproduces this distribution reasonably well (Fig. 5h). However, it underestimates the areal average (Table 1). The spatial correlation (0.55) is larger than that of spring but smaller that those of winter and summer. Winds at 850 hPa in this season are northwesterly in the AS and westerly/northwesterly in other seas. The model simulates the wind pattern fairly well, but it generally simulates stronger winds than those in the forcing data.

Overall, it could be said that the model is capable of reproducing the seasonal amount and distribution of the precipitation in the AP. Therefore, its performance could be assumed to be sufficient to carry out sensitivity simulations to explore the effect of SST changes on the precipitation of the AP.

4 Results

4.1 Aegean Sea

The AS is the smallest of the three seas considered in this study. Nevertheless, its significance lies in the fact that it is located in the upwind side of the AP, especially in winter and spring (see Fig. 5). According to Karaca et al. (2000), the AS possesses at least two major cyclone trajectories: One crosses the AS zonally and moves eastward following a path over Anatolian Plateau between two mountain ranges, North Anatolian and Taurus, and the other crosses the sea diagonally and moves towards the western BS following a track over the Sea of Marmara and the surrounding lowlands. The cyclones following both paths cause substantial precipitation in western and northwestern parts of the AP.

Figure 6 shows seasonal precipitation differences between the sensitivity and control simulations for the AS. In general, increasing SSTs of the AS causes increase in precipitation at the sea basin itself and the surrounding coastal areas. The changes extend to the inland areas in the western parts of the AP in winter, spring and autumn. There are areas in both sea and land where the changes in precipitation are statistically significant at 95% confidence level. In winter (Fig. 6a), statistically significant areas lie in the southeastern half of the AS and southern parts of the western coastal line of the AP. In spring (Fig. 6b), majority of the precipitation increases in the AS is statistically significant. On the land, mostly those along the western coastline of the AP are significant at 95% confidence level. There are few grids with significant increase in precipitation in summer (Fig. 6c). There are many in autumn, but few of them are on the land (Fig. 6d). It should be noted here that there are many large as well as small islands in the AS, and it seems that an increase in the SSTs of the AS has the potential to increase the precipitation these islands receive.

As mentioned earlier, relatively strong northwesterly and westerly winds dominate the airflow at 850 hPa level over the AS in winter and spring. This airflow that is subject to modifications over the AS by the increased SSTs results in significant increases in precipitation downwind, in the coastal regions in the western parts of the AP. In summer, there is either little increase or no change in precipitation in the basin since very dry and warm atmospheric conditions associated with the anticyclonic circulation dominate the weather in this region. In autumn, 850 hPa winds over the AS start to take westerly component. In this season, the trajectories of the cyclonic systems

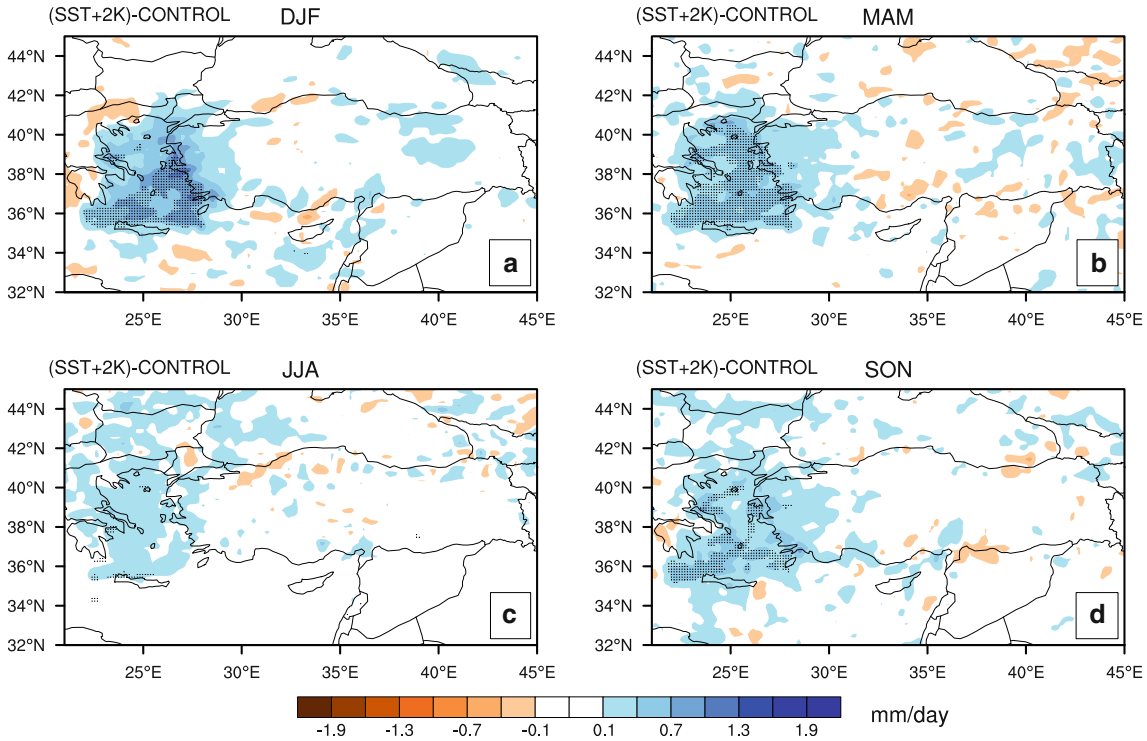

Fig. 6 10-year average precipitation differences between the Aegean Sea sensitivity simulation (SST + 2 K) and the control simulation for winter (DJF) (**a**), for spring (MAM) (**b**), for summer (JJA) (**c**) and for autumn (SON) (**d**). Hatching is for significant changes at 95% confidence level

gradually shift southward and these systems start to influence the AS basin. Therefore, the role of SST changes on the precipitation increases again, though not as strong as that in winter and spring.

4.2 Eastern Mediterranean Sea

The EMS covers the eastern flank of the Mediterranean Sea, and it is much larger than the AS. The 850 hPa level wind vectors indicate westerly and northwesterly airflow over the EMS in all seasons (see Fig. 5). From time to time in the cold half of the year, cyclonic systems that originate from the northern Atlantic Ocean take a southerly trajectory, especially when the Azores high is weak (which is usually indicated by a negative North Atlantic Oscillation index), and they move over the western Mediterranean Sea where they gain strength from below through evaporation. Then, they move eastward and pass over the EMS, Lebanon, Syria, southeastern and eastern parts of the AP. These systems produce substantial precipitation on the sea facing sides of Taurus mountain range in the southern parts of the AP and the mountains along the coasts of Lebanon and Syria. Because the prevailing winds are predominantly westerly, the west looking sides along the coastline receive more precipitation than the east looking sides. There are some situations in which the location of a low-pressure system allows its cyclonic circulation enough fetch distance over the EMS to pick moisture in large quantities. In such cases, the moisture-laden southerly winds in the eastern side of such systems cause severe precipitation events in the bay areas along the EMS coasts of the AP.

As in the AS case, increasing SSTs of the EMS enhance the precipitation in the test-bed region in all seasons (Fig. 7). In addition, it increases the precipitation along the coastal areas in the north and east and the vast inland areas in the eastern Anatolian highlands. In winter (Fig. 7a), the increases across the EMS including the island of Cyprus are statistically significant at the 95% confidence level. There are large areas on the land with statistically significant increases as well. Their northeastern orientation also suggests the favorable track for the east Mediterranean storms that affect eastern Anatolia. It seems that the SST increases in the EMS have the potential to increase precipitation significantly in the headwaters of the Euphrates river basin (Fig. 7a). Apart from these changes, the SST increase in the EMS has a tendency to decrease precipitation in the AS. The reductions are significant in a few grids in the southeastern part of the AS.

In both spring (Fig. 7b) and autumn (Fig. 7d), the areal extent of the increases in precipitation is somewhat

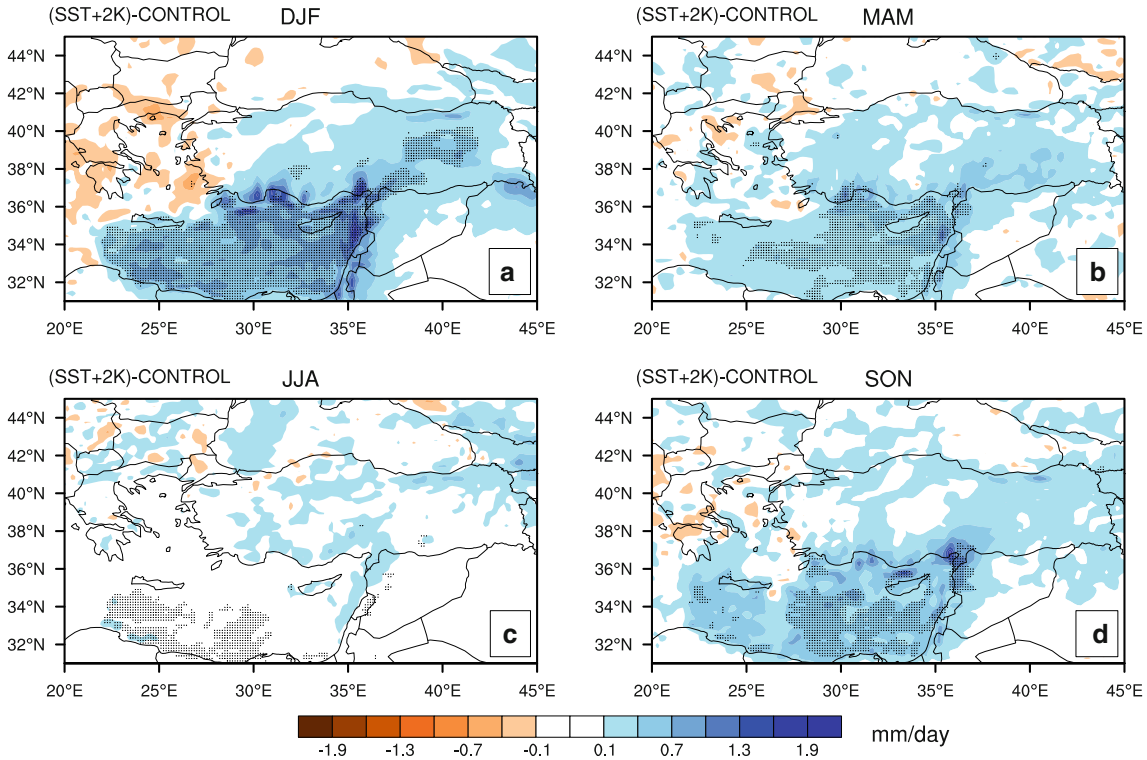

Fig. 7 10-year average precipitation differences between the eastern Mediterranean Sea sensitivity simulation (SST + 2 K) and the control simulation for winter (DJF) (**a**), for spring (MAM) (**b**), for summer (JJA) (**c**) and for autumn (SON) (**d**). Hatching is for significant changes at 95% confidence level

similar to that in winter, but the magnitudes of the changes are usually small. Statistically significant grids spread generally to the eastern portions of the EMS in spring, and southeastern portions in autumn. Unlike that in winter, the precipitation increases in the island of Cyprus are mostly insignificant in both seasons. There are few grids with the significant increases in the inland areas of the AP, but there are many along its southern coasts. The increases in the coastal regions of Syria are also significant in both spring and autumn. The impact of SST increases in the EMS is comparatively small in the AP in summer (Fig. 7c). The statistically significant increases, especially those in the southwestern portions of the EMS, are most likely related to the enhanced convective activity in these areas.

4.3 Black Sea

The BS is a bit smaller than the EMS but almost twice the size of the AS. It forms a pretty long coastline in the north with the AP. The 850 hPa wind vectors (see Fig. 5) illustrate mostly westerly airflow over the BS in winter, spring and autumn. The airflow is predominantly northerly in summer, which helps keep the northern parts of the AP relatively wet in this season (Fig. 5c). The cyclonic circulation over the eastern BS is also an important seasonal feature resulting in high rainfall amounts in the surrounding lands in summer.

The basinwide precipitation enhances in response to the increased SSTs in the BS in all seasons (Fig. 8). Surprisingly, there are few grids on the sea with statistically significant increases in winter and spring (Fig. 8a, b). On the other hand, statistically significant grids cover large portions of the BS in both summer and autumn (Fig. 8c, d). Precipitation of the surrounding lands is also positively influenced by the increases in the SSTs, however, the changes are generally insignificant at the 95% confidence level. In the AP, the increases in precipitation are mostly confined to a narrow band along the land–sea boundary in all seasons. In summer, this band is a little bit wider, and there are two relatively large spots in the central and eastern parts where the increases are statistically significant. The central parts of the AP seem to be broadly unaffected by the increases in the SSTs of the BS.

4.4 The seas together

The AS is considered a part of the Mediterranean Sea whereas the BS is generally not, despite their connection through Bosporus and Dardanelles Straits. Indeed, seasonally averaged SSTs of the AS are very close (1–3°C cooler) to those of the EMS. Moreover, there is a high

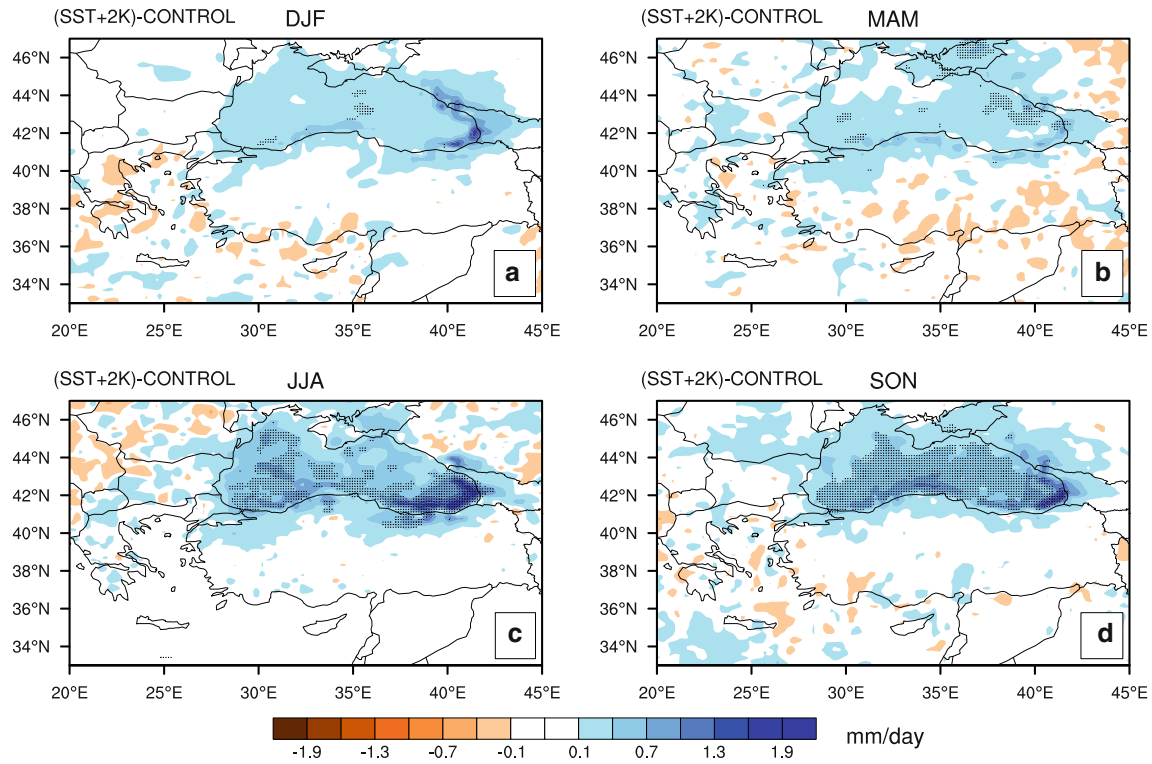

Fig. 8 10-year average precipitation differences between the Black Sea sensitivity simulation (SST + 2 K) and the control simulation for winter (DJF) (**a**), for spring (MAM) (**b**), for summer (JJA) (**c**) and for autumn (SON) (**d**). Hatching is for significant changes at 95% confidence level

co-variability in the temporal evolution of their SSTs (see Fig. 2). The SSTs of the BS are much lower (3–9°C on seasonal basis) than those of the EMS, however, there is still some consistency in their year-to-year and decadal variability (see Fig. 2). It could be said that because the SST variability of the three seas is somewhat related any change in the SSTs in this region is likely to take place in all these seas rather than individual ones as treated so far. Therefore, it is imperative to check the combined effect of the SST changes in all seas on the precipitation of the AP.

We conducted a fourth sensitivity simulation and simultaneously changed the SSTs of all the seas surrounding the peninsula by +2 K. Figure 9 shows the 10-year seasonal average differences in precipitation between this simulation and the control one. As in other sensitivity simulations, precipitation increases in the three seas in response to the increased SSTs. Furthermore, it increases all over the AP in all seasons. It seems that the combined effect is a bit more pronounced version of the sum of the individual effects. In winter (Fig. 9a), the areas with the statistically significant changes seem to be depicted by the changes caused by the EMS. Almost all the precipitation changes in the EMS are significant. Note that the negative sensitivity of the AS basin to the increased SSTs in the EMS decreases the statistically significant area that is obtained in the AS sensitivity simulation. The changes in the BS are more or less similar to those acquired in its single simulation, and adding the other seas to the sensitivity simulation does not make any remarkable change in the precipitation falling in the sea. The significant changes in the AP in winter seem to be dominated by the changes caused by the increased SSTs in the EMS. Taking other seas into account slightly increases the extension of the areas with statistically significant changes. These areas are important for the water resources in the AP as they feed the vital rivers in the region such as the Euphrates.

In spring (Fig. 9b), again, the effect of the seas altogether looks more like the sum of their individual effects. Perhaps, the most important difference is that there are more patches in the AP with statistically significant increases in precipitation. They are not only located in the coastal areas but also in the interior regions. The sensitivity simulations that treated the seas individually yielded that it was the BS that was the most influential on the precipitation of the AP in summer. This is more or less the case when all three seas are taken into account in the same simulation (Fig. 9c). Substantial increases occur along a band parallel to the BS coastline of the AP, and the areas with significant increases are located in the central and eastern portions of this band. The SST increases in all three seas surrounding the AP enhance the precipitation all over the peninsula in autumn, but the changes are significant at a

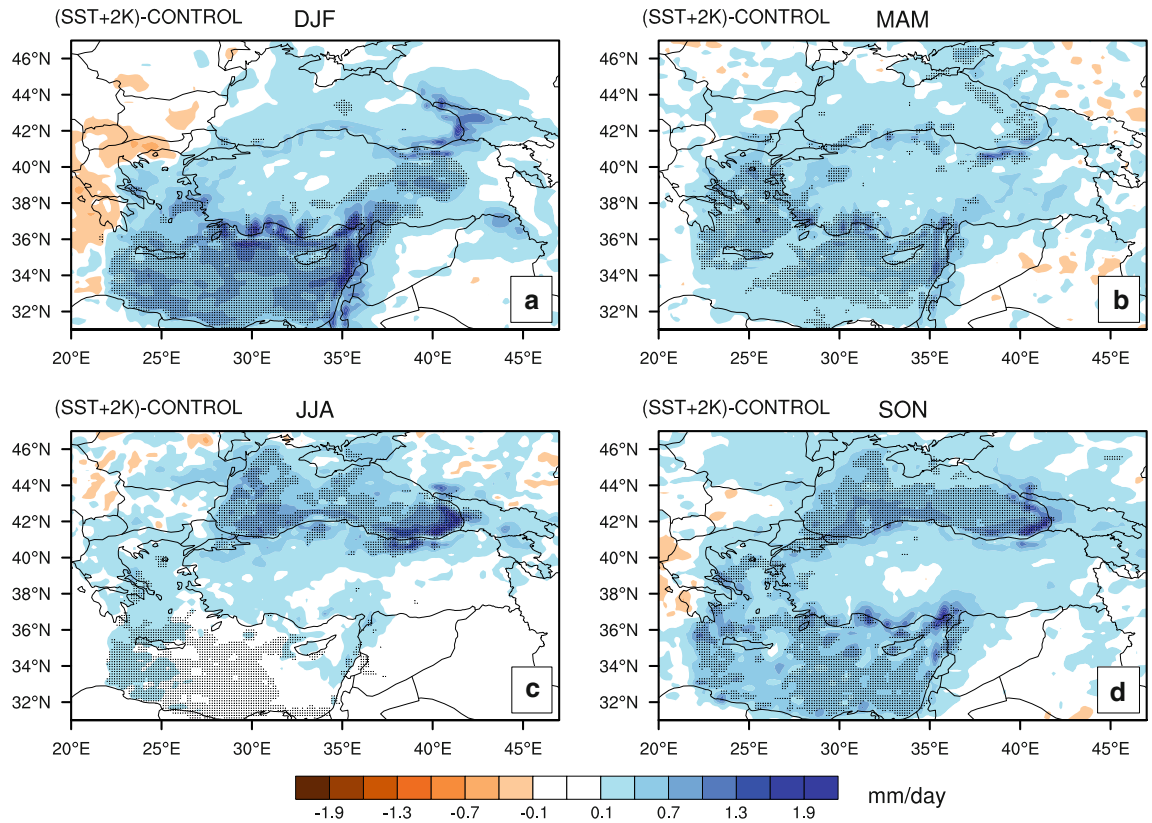

Fig. 9 10-year average precipitation differences between all-the-seas sensitivity simulation (SST + 2 K) and the control simulation for winter (DJF) (**a**), for spring (MAM) (**b**), for summer (JJA) (**c**) and for autumn (SON) (**d**). Hatching is for significant changes at 95% confidence level

very few locations (Fig. 9d). Perhaps, the most important increase takes place in the land towards the Bosporus Strait, a densely populated part of the peninsula.

This experiment indicates that the changes in the SSTs of the three seas around the AP may cause substantial changes in the precipitation of the peninsula, some of which are statistically significant. To understand how this happens, we looked into the changes in other surface and upper atmospheric variables. As can be expected, increasing SSTs increases energy fluxes from the sea surface (not shown here). The magnitudes of the increases are not uniform across the seas, and the changes are typically larger in the upwind side. Also, the increases in the latent heat flux are generally 2–3 times larger than those in the sensible heat fluxes. Because more heat energy is transferred to the atmosphere, the height of the planetary boundary layer increases over the seas. Figure 10 illustrates the seasonal changes in the 850 hPa level wind magnitude and geopotential height. There are some consistent changes in the 850 hPa wind magnitude in all seasons. There is a general tendency for winds at this level to become stronger over the EMS and AS while weaker over the western Anatolia and the BS except its southeastern parts where they tend to get stronger in response to the increased SSTs. This pattern, which is especially well established in winter, indicates the existence of two cyclonic anomalies, a large one centered around the northern EMS and a relatively small one centered around the eastern BS. These anomalies are also well depicted by the reductions in the geopotential height. It is obvious that such changes in the wind fields enhance the transport of moister and warmer air from the EMS to the eastern Anatolia.

Figure 11 shows the seasonal changes in the 850 hPa moist static energy. The moist static energy at this level increases over the AP as well as over the three seas in all seasons. Apparently, the increases are larger over the downwind sides of the seas. The largest increases over the AP occur along a band extending from EMS to eastern BS in winter. This band coincides well with the areas that have significant increases in precipitation (see Fig. 9a). The distribution of the moist static energy difference in spring is similar to that one in winter, but the increases are smaller in magnitude. In summer, the largest increases in moist static energy occur over the lands that are in the downwind side of the seas. The increase over the northern parts of the AP where the precipitation increases is especially noteworthy. In autumn, the transport of moist static energy over

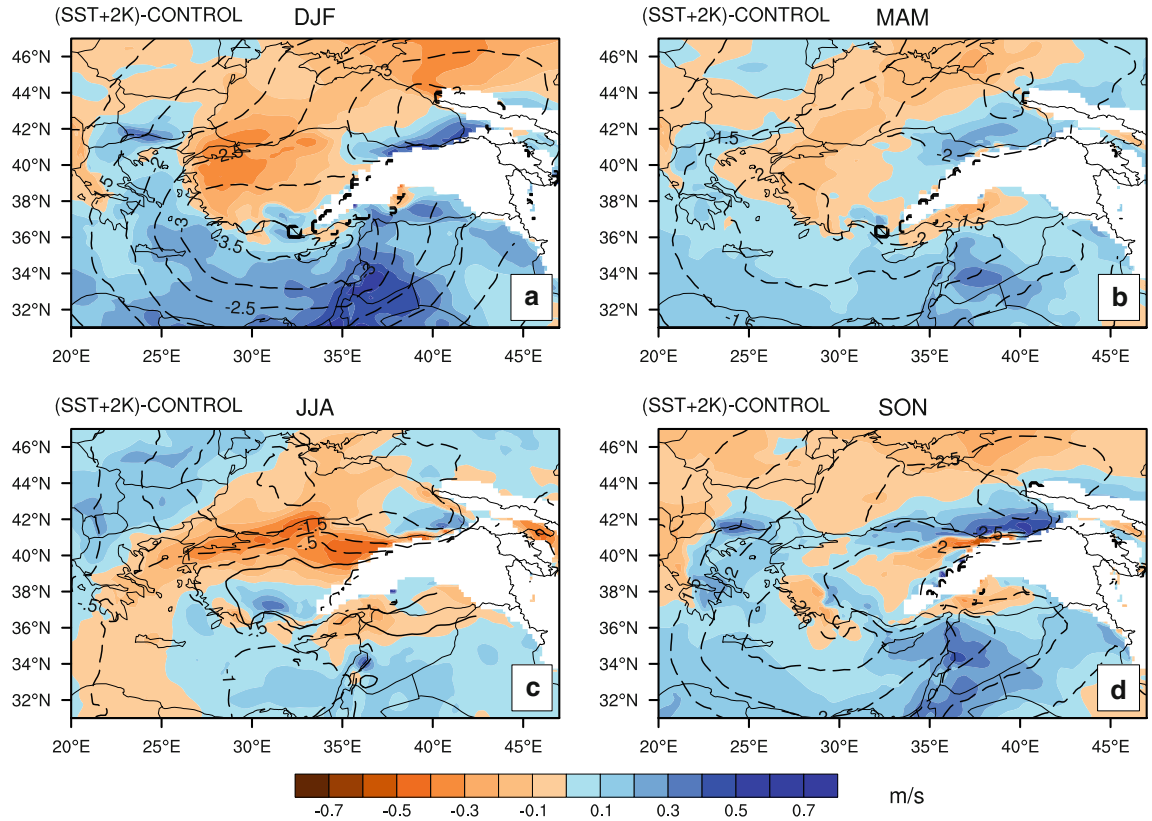

Fig. 10 10-year average 850 hPa wind magnitude (*background color pattern* in units of m/s) and geopotential height (*contour lines* in units of gpm) differences between all-the-seas sensitivity simulation (SST + 2 K) and the control simulation for winter (DJF) (**a**), for spring (MAM) (**b**), for summer (JJA) (**c**) and for autumn (SON) (**d**). Contour line interval is 0.5 gpm and negative differences are *dashed*

the AP is also enhanced in response to the increased SSTs. The areal coverage of the changes looks more like a combination of those of the winter and summer.

From the analysis of the changes in these and other surface and atmospheric variables, it is possible to hypothesize a mechanism that may explain the link between the SST increase around the AP and the change in regional precipitation. Increasing SSTs cause more transfer of heat and moisture from the sea surface to the atmosphere. The additional heat energy makes the boundary layer warmer, and increases its height over the seas. It also enhances the convection. Indeed, the convective precipitation increases in the AS and EMS in winter, in the BS in summer, and in all the seas in the transition seasons. If summer is excluded, the increases in the convective precipitation are usually small in the AP in other seasons, and therefore, they account for a small fraction of the change in the total precipitation. This means that the increases in the AP are predominantly coming from the increases in the precipitation that is caused by the large-scale circulation. The additional moisture gained over the seas by the overpassing air masses in response to the increased SSTs is transported over the land where it enhances the precipitation triggered by the orography and frontal activity. The evidence of the moisture transport is the increased humidity over the AP, which is not shown here but clearly implied by the increases in the moist static energy illustrated in Fig. 11. In addition to moisture, the air circulation carries heat energy from over the seas to over the land areas. This is especially important for the eastern Anatolia that is covered by snow for months. The additional heat causes earlier melting of the snow cover. Nevertheless, when we checked the daily differences in the snow water equivalent between the sensitivity (including all three seas) and control simulations for a box in the eastern Anatolia, we observed up to 10–15% increases in this parameter, which is a result of the increase in winter precipitation.

5 Summary and discussion

This study investigates the effects of the warmer SSTs in the surrounding seas of the Anatolian Peninsula on its precipitation through sensitivity simulations using a state-of-the-art regional climate model, RegCM3. The analysis is based on one reference simulation with the observed SSTs (Reynolds et al. 2002) and four sensitivity simulations in which a 2-K increase is applied to the SSTs of the Aegean,

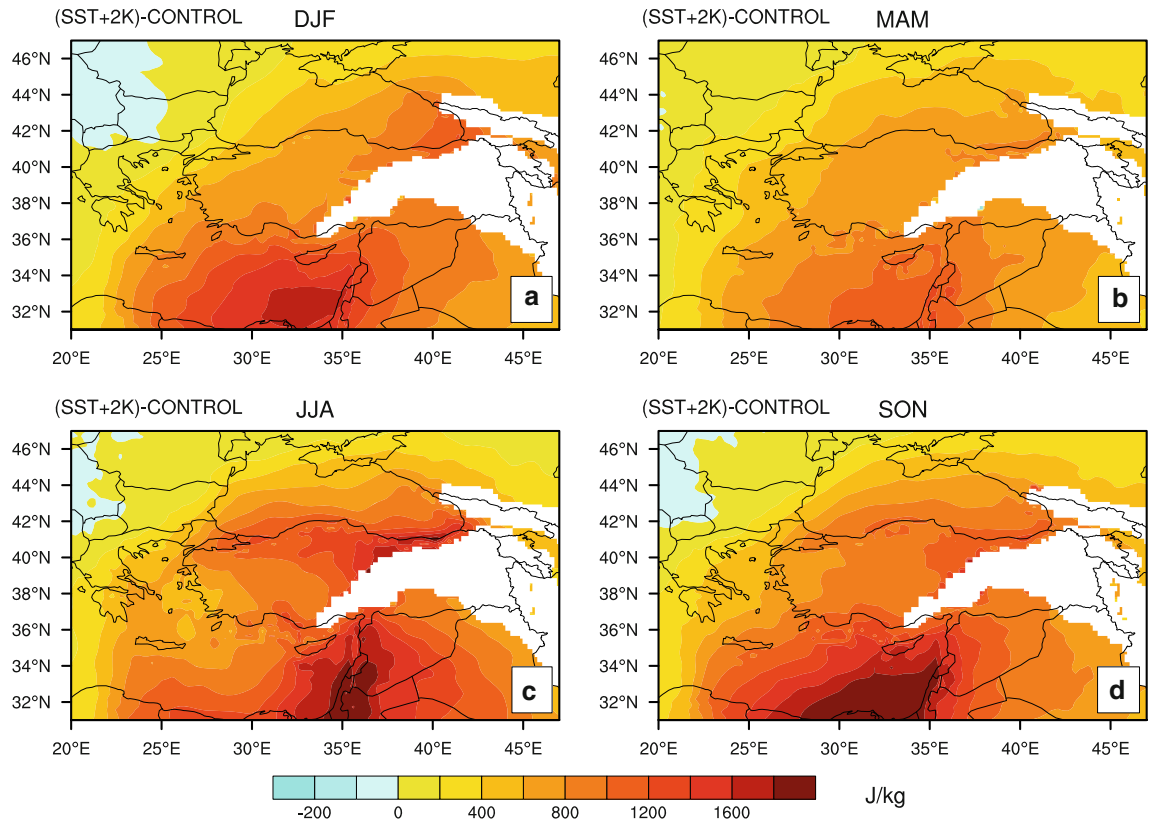

Fig. 11 10-year average 850 hPa moist static energy (J/kg) differences between all-the-seas simulation (SST + 2 K) and the control simulation for winter (DJF) (**a**), for spring (MAM) (**b**), for summer (JJA) (**c**) and for autumn (SON) (**d**)

eastern Mediterranean and Black seas individually as well as collectively. All the simulations are integrated over a 10-year period between 1990 and 2000. The performance analysis of the control simulation indicates that the model is capable of reproducing the seasonal amounts and distribution of the precipitation in the Anatolian Peninsula reasonably well.

A statistical analysis in a preliminary work to this study revealed poor correlations between the time series of the precipitation of the stations in the Anatolian Peninsula and the SSTs of the surrounding seas (Similar results are also found by Barret 2006). The model simulations of this study, however, indicate that the precipitation of the peninsula is sensitive to the variations of the SSTs of these seas. It is clear from the sensitivity simulations that, in general, warmer SSTs lead to increases in the precipitation of the peninsula as well as that of the seas considered. Not all the changes are significant at 95% confidence level though. The statistically significant increases at this level largely occur in the seas where SSTs are modified, and along the coastal areas that are in the downwind side. Significant increases do take place in the interior areas of the peninsula as well. The simulations reveal that eastern Mediterranean Sea has the biggest potential to affect the precipitation in the peninsula. They also demonstrate that taking all three seas into account simultaneously enhances the effect of SSTs on the peninsula's precipitation, and extends the areas with statistically significant increases.

The Anatolian Peninsula receives most of its precipitation in winter, usually in the form of snow. Starting from late October and early November, snow accumulates in the eastern parts of the peninsula where important rivers such as Euphrates, Tigres, Aras and Kızılırmak originate. Substantial melting in the region begins late February and early March with the increase of temperature caused by the warmer airflow coming from the eastern Mediterranean Sea. The sensitivity simulations indicate that the additional heat and moisture gained over the warmer eastern Mediterranean Sea are carried over the eastern Anatolia. The moisture advection makes significant increases in the winter precipitation in large areas in the region, which are the headwaters of the Euphrates and Kızılırmak rivers. The heat advection, on the other hand, leads to increases in the surface temperatures. For the cold half of the year, the increases in the daily mean temperatures averaged for a box in the region vary around 0.3 K in the case of eastern Mediterranean Sea experiment and 0.5 K in the case of all seas considered. There is no doubt that such increases in

temperature, though small, may contribute to the snowmelt process, and therefore, may have important implications for the water resources of the region.

The sensitivity simulations of this study could be evaluated within the context of climate change issue as well. Climate change projections based on the IPCC's worst-case scenarios (e.g., A2 and A1FI) estimate up to around 6°C increases in the surface temperatures of the Anatolian Peninsula by the end of the twenty-first century (e.g., Onol and Semazzi 2009). As shown in Fig. 3, the projections also foresee up to around 4°C increases in the SSTs of the surrounding seas of the peninsula. Despite such increases in SSTs, they indicate large reductions in precipitation over eastern Mediterranean including southern and western parts of the peninsula (Giorgi and Lionello 2008; Onol and Semazzi 2009). This seems contrary to the findings in the present study. As mentioned earlier, the drying of the large Mediterranean Basin is related to the strengthening of the anticyclonic circulation and poleward shift of the Atlantic cyclone tracks (Musculus and Jacob 2005; Lionello and Giorgi 2007). Thus, it can be said that the basinwide reduction of the precipitation in the Mediterranean is a result of the changes in the continental—perhaps global—scale circulation in response to the enhanced greenhouse gasses. It seems that the rising motions that may be induced by the increase in the SSTs in the Mediterranean Sea are suppressed by the strengthening of the anticyclonic circulation. Another important point to mention is that the difference between the temperatures of the sea surface and atmosphere (say for instance 850 hPa level) may be reduced in the climate change simulations as implied by the temperature increases given above. This may lead to a decrease in the heat flux to the atmosphere. In the present study, however, increasing SSTs clearly increase surface-atmosphere temperature gradient causing greater heat flux to the atmosphere. This enhances the instability and rising motions over the seas that facilitate the transfer of water vapor from the sea surface to the atmosphere.

The present study reveals an interesting feature for the seas surrounding the Anatolian Peninsula: The Black Sea behaves differently in many ways compared to the other seas. Its precipitation has little or no significant response to the increased SSTs in winter and spring while those of the Aegean and eastern Mediterranean seas show strong sensitivity in the same seasons. Moreover, this is more or less true in terms of their influence on the precipitation of the peninsula. The latter may be related to the fact that the prevailing winds are usually westerly over the Black Sea in these seasons. This means that the air flows parallel to or away from the Black Sea coastline of the peninsula. Despite the prevailing wind direction, easterly and northeasterly winds blow over the Black Sea when the Siberian High occasionally extends towards Europe. Such winds bring over cold air to the western and southwestern Black Sea where they meet with the warmer and moister air coming from the south. In such cases, the cold air may gain substantial moisture while travelling over the Black Sea especially when the fetch distance is relatively long. Such events may generate considerable amounts of precipitation, mostly in the form of snow, in the western Black sea and the lands to the south. They may also cause occasional sea effect snow events around the city of Istanbul (Kindap 2009).

The Black Sea also demonstrates notable differences in summer compared to the others. The effect of the Black Sea on the precipitation of both its basin and the Anatolian Peninsula increases while the effects of the other seas decrease. The response of autumn precipitation to the increased SSTs is comparatively strong in the Black Sea as well. There is no doubt that the northerly wind direction in summer and the enhanced convection in both summer and autumn play important roles in the occurrence of these changes. The most densely populated and industrialized areas of the Anatolian Peninsula lie in the northwestern parts including the city of Istanbul, which has a population of over 12 millions. The changes in the precipitation of this area are therefore very important. It seems that it is the Black Sea that has the largest potential to affect the precipitation of this area. The increase in the SSTs of the Black Sea tends to enhance the precipitation there in all seasons. The increases in summer and autumn amount to the levels that are statistically significant at 95% confidence level. When the SST change is applied to the all seas simultaneously, the statically significant area becomes larger in that region, especially in autumn.

In line with the results of the present study, majority of the climate change simulations estimate increasing tendencies in the precipitation of the northeastern coastal areas of the Anatolian Peninsula (e.g., Onol and Semazzi 2009). This region already receives high amounts of precipitation (over 2,000 mm), and for this and other reasons (steep topography, conversion of forest areas to tea plantations, etc.), the region is prone to frequent landslide occurrence. It could be said that the increase in the precipitation of the region in response to the increased SSTs will result in the rise of the likelihood of the landslide occurrence.

It should be noted that increasing SSTs enhances the convective activity over the seas. As a result, convective precipitation increases in the seas, but it also increases in the coastal areas of the Anatolian Peninsula. It is likely that warmer summer and autumn SSTs of the surrounding seas of the peninsula enhance the formation of the flash floods, torrential precipitation events and tornado-like systems especially in the southwest Black Sea (e.g., Efimov et al. 2008) and also the sea facing sides of the mountains that are located in the southern parts of the peninsula. Also, the

formation of extreme precipitation events depends strongly on the favorable synoptic situations and atmospheric circulations (Lenderink et al. 2008). The west looking sides of the mountain ranges along the Mediterranean coast of the Anatolian Peninsula receive the highest annual precipitation as the prevailing westerlies carry moisture–laden air towards them yearlong. What's interesting is that the severe precipitation events that produce maximum daily rainfall amounts take place in the areas towards the east looking sides of the mountain ranges. This is basically because the fetch distance over the sea for the winds that are associated with a cyclone whose center is located in the west of the area is maximized. This allows the moving air to pick substantial amounts of heat and moisture from the sea surface. Because of the cyclonic circulation, the winds become southerly when they reach to the southern coasts of the Anatolian Peninsula. Such situations generate torrential rainfall events in the east looking sides of the mountain ranges. Needles to say that increasing SSTs of the Aegean and eastern Mediterranean seas will strengthen such systems by providing more heat and moisture. The result will be more devastating precipitation events in such areas.

The results of this sensitivity study are more or less related to the climatology, but the response of precipitation to SST in cases of individual precipitation events could be very different. Further study is needed to address the relationship between individual severe precipitation events in the Anatolian Peninsula and the changes in the SSTs of the surrounding seas. Furthermore, it will be interesting to study the cyclones affecting the peninsula in conjunction with their interactions with the surrounding seas.

Acknowledgments This study is partly supported by grants (105Y341 and 106G015) from TUBITAK (The Scientific and Technological Research Council of Turkey). The simulations were performed at the National Center for High Performance Computing at the Istanbul Technical University. The authors are grateful to two anonymous reviewers for their constructive comments, which helped improve the manuscript.

References

Anthes RA (1977) A cumulus parameterization scheme utilizing a one-dimensional cloud model. Mon Weather Rev 105:270–286

Arpe K, Dümenil L, Giorgetta MA (1998) Variability of Indian Monsoon in the ECHAM3 Model: sensitivity to sea surface temperature, soil moisture, and stratospheric quasi-biennial oscillation. J Clim 11:1837–1858

Barret BS (2006) Relationship between sea surface temperature anomalies and precipitation across Turkey. In: Unal Y, Kahya C, Bari DD (eds) Proceedings of the International Conference on Climate Change and the Middle East: past, present and future. Istanbul Technical University, Istanbul

Bolle HJ (ed) (2003) Mediterranean climate—variability and trends. Springer, Berlin, p 372

Bozkurt D, Sen OL, Turuncoglu UU, Karaca M, Dalfes HN (2008) Regional climate change projections for Eastern Mediterranean: preliminary results, vol 10, EGU2008-A-04264

Bozkurt D, Sen OL, Karaca M (2009) Performance of RegCM3 over a mountainous region in the Eastern Mediterranean (in prep.)

Brody LR, Nestor MJR (1980) Regional forecasting aids for the Mediterranean Basin. In: Handbook for forecasters in the Mediterranean, part 2. Technical Report TR 80-10, Naval Environmental Prediction Research Facility, Monterey, California, pp 1–13

Dickinson RE, Henderson-Sellers A, Kennedy PJ (1993) Biosphere-atmosphere transfer scheme (BATS) version 1e as coupled to the NCAR community climate model. Tech Note TN-387+STR, NCAR, pp 72

Efimov VV, Stanichnyi SV, Shokurov MV, Yarovaya DA (2008) Observations of a quasi-tropical cyclone over the Black Sea. Russ Meteorol and Hydrol 33(4):233–239

Emanuel KA, Zivkovic-Rothman M (1999) Development and evaluation of a convection scheme for use in climate models. J Atmos Sci 56:1766–1782

Evans JP (2009) 21st century climate change in the Middle East. Clim Change 92:417–432

Gao X, Pal JS, Giorgi F (2006) Projected changes in mean and extreme precipitation over the Mediterranean region from high resolution double nested RCM simulations. Geophys Res Lett 33:L03706

Giorgi F, Lionello P (2008) Climate change projections for the Mediterranean region. Glob Planet Chang 63:90–104

Giorgi F, Bates GT, Nieman SJ (1993a) The multi-year surface climatology of a regional atmospheric model over the western United States. J Clim 6:75–95

Giorgi F, Marinucci MR, Bates GT, DeCanio G (1993b) Development of a second generation regional climate model (RegCM2). Part II: convective processes and assimilation of lateral boundary conditions. Mon Weather Rev 121:2814–2832

Gokturk OM, Bozkurt D, Sen OL, Karaca M (2008) Quality control and homogeneity of Turkish precipitation data. Hydrol Process 22(16):3210–3218

Grell G (1993) Prognostic evaluation of assumptions used by cumulus parameterization. Mon Wea Rev 121:764–787

Holtslag AAM, DeBruijn EIF, Pan HL (1990) A high resolution air mass transformation model for short range weather forecasting. Mon Wea Rev 118:1561–1575

Hsie EY, Anthes RA, Keyser D (1984) Numerical simulation of frontogenesis in a moist atmosphere. J Atmos Sci 41:2581–2594

IPCC (2007) Intergovernmental Panel on Climate Change fourth assessment report on scientific aspects of climate change for researchers, students, and policymakers

Janicot S, Harzallah A, Fontaine B, Moron V (1998) West African monsoon dynamics and Eastern Equatorial Atlantic and Pacific SST anomalies (1970–1988). J Clim 11:1874–1882

Karaca M, Deniz A, Tayanc M (2000) Cyclone track variability over Turkey in association with regional climate. Int J Climatol 20:122–136

Kiehl JT, Hack JJ, Bonan GB, Boville BA, Briegleb BP, Williamson DL, Rasch PJ (1996) Description of the NCAR Community Climate Model (CCM3). NCAR Technical Note, NCAR/TN-420+STR, pp 152

Kindap T (2009) A severe sea-effect snow episode over the city of Istanbul. Nat Hazards (in review)

Lenderink G, van Meijgaard E, Selten F (2008) Intense coastal rainfall in the Netherlands in response to high sea surface temperatures: analysis of the event of August 2006 from the perspective of a changing climate. Clim Dyn. doi: 10.1007/s00382-008-0366-x

Li LZX (2006) Atmospheric GCM response to an idealized anomaly of the Mediterranean sea surface temperature. Clim Dyn 27: 543–552

Lionello P, Giorgi F (2007) Winter precipitation and cyclones in the Mediterranean region: future climate scenarios in a regional simulation. Adv Geosci 12:153–158

Lionello P, Bhend J, Buzzi A, Della-Marta PM, Krichak S, Jansa A, Maheras P, Sanna A, Trigo IF, Trigo R (2006) Cyclones in the Mediterranean region: climatology and effects on the environment. In: Lionello P, Malanotte-Rizzoli P, Boscolo R (eds) Mediterranean climate variability. Elsevier, Amsterdam, pp 324–372

Maheras P, Flocas H, Patrikas I, Anagnostopoulou C (2001) A 40 year objective climatology of surface cyclones in the Mediterranean region: patial and temporal distribution. Int J Climatol 21:109–130

Maracchi G, Crisci A, Grifoni D, Gozzini B, Meneguzzo F (1999) Relationships between extreme convective events and sea surface temperature anomalies in coastal regions of the Mediterranean. Proceedings of the EuroConference on global change and catastrophe risk management: flood risks in Europe. Laxenburg, Austria

Messager C, Gallee H, Brasseur O (2004) Precipitation sensitivity to regional SST in a regional climate simulation during the West African monsoon for two dry years. Clim Dyn 22:249–266

Musculus M, Jacob D (2005) Tracking cyclones in regional model data: the future of Mediterranean storms. Adv Geosci 2:13–19

Onol B, Semazzi FHM (2009) Regionalization of climate change simulations over Eastern Mediterranean. J Clim 22:1944–1961

Pal JS, Smal EE, Eltahir EAB (2000) Simulation of regional-scale water and energy budgets: representation of subgrid cloud and precipitation processes within RegCM. J Geophys Res 105(D24):29579–29594. doi:10.1029/2000JD900415

Pal JS, Giorgi F, Bi X et al (2007) Regional climate modeling for the developing world: the ICTP RegCM3 and RegCNET. Bull Am Meteorol Soc 88(9):1395–1409

Reynolds RW, Rayner NA, Smith TM, Stokes DC, Wang W (2002) An improved in situ and satellite SST analysis for climate. J Clim 15:1609–1625

Rodo X, Baert E, Fa Comin (1997) Variations in seasonal rainfall in southern Europe during the present century: relationships with the North Atlantic Oscillation and the El Nino Southern Oscillation. Clim Dyn 13:275–284

Romem M, Ziv B, Saaroni H (2007) Scenarios in the development of Mediterranean cyclones. Adv Geosci 12:59–65

Rowell DP (2003) The impact of Mediterranean SSTs on the Sahelian rainfall season. J Clim 16:849–862

Tayanc M, Karaca M, Dalfes HN (1998) March 1987 Cyclone (Blizzard) over the Eastern Mediterranean and Balkan region associated with blocking. Mon Weather Rev 126:3036–3047

Trigo IF, Davies TD, Bigg GR (2000) Decline in Mediterranean rainfall caused by weakening of Mediterranean cyclones. Geophys Res Lett 27:2913–2916

Trigo R et al (2006) Relations between variability in the Mediterranean region and mid-latitude variability (lead author of Chapter 3). In: Lionello P, Malanotte-Rizzoli P, Boscolo R et al (eds) The Mediterranean climate: an overview of the main characteristics and issues. Elsevier, Amsterdam, pp 179–226

Wang Y, Sen OL, Wang B (2003) A highly resolved regional climate model (IPRC_RegCM) and its simulation of the 1998 severe precipitation events over China. J Clim 16:1721–1738

Xoplaki E, González-Rouco JF, Luterbacher J, Wanner H (2004) Wet season Mediterranean precipitation variability: influence of large-scale dynamics and trends. Clim Dyn 23:63–78

Zeng X, Zhao M, Dickinson RE (1998) Intercomparison of bulk aerodynamic algorithms for the computation of sea surface fluxes using TOGA COARE and TAO data. J Clim 11:2628–2644